aerospace

Article

Life Cycle Assessment of the Cellulosic Jet Fuel Derived from Agriculture Residue

Ziyu Liu [1], Haobo Liu [1] and Xiaoyi Yang [2,*]

[1] School of Aeronautic Science and Engineering, Beihang University, Beijing 100191, China
[2] School of Energy and Power Engineering, Energy and Environment International Centre, Beihang University, Beijing 100191, China
* Correspondence: yangxiaoyi@buaa.edu.cn

Abstract: The purpose of this paper is to discover the impacts of contradictory factors in the application of agricultural residue with sustainable biofuel benefits. Based on the Life cycle assessment (LCA) approach, the quantitative LCA assessment model and approach have been established, coupling upstream cultivation and downstream jet biofuel product, which would benefit agriculture residue choice. The LCA model investigated the effects of interaction factors on energy consumption, including land release and agriculture residue use change. The computational framework of the LCA model is classified into three sub-models, including the cultivation and harvesting model, the refining process and distribution model, and the flight model. According to uncertainty analysis by the LCA model, the positive energy gains have been conducted at a wide range of hydrogen production and methanol production. The application model is represented by six types of typical aircraft widely used in China, including the LTO cycle module, actual cruising distance and maximum cruising distance module, actual payload, and maximum payload module. In the whole life cycle assessment, GHGs of agriculture residue is 17.9 gCO_2e/MJ while petroleum-based jet fuel is 90.2 gCO_2e/MJ. The order of GHGs in WTW (well to wheel) is agriculture residue < corn stover < beanstalk < wheat straw < rice straw. The land release conducted obviously to the total GHGs emission for rice straw, which indicated that land release should involve in the LCA.

Keywords: CO_2 sequestration; uncertainty analysis; LCA; biodiesel; Algae; jet biofuel

check for updates

Citation: Liu, Z.; Liu, H.; Yang, X. Life Cycle Assessment of the Cellulosic Jet Fuel Derived from Agriculture Residue. *Aerospace* **2023**, *10*, 129. https://doi.org/10.3390/aerospace10020129

Academic Editors: Daochun Li, Ting Li, Weizong Wang, Xiaoqiang Li, Zhenxun Gao, Zhihua Wang, Lizhan Bai and Zhan Tu

Received: 30 August 2022
Revised: 4 November 2022
Accepted: 7 November 2022
Published: 31 January 2023

1. Introduction

Green aviation makes an important impact on global carbon reduction and the control of greenhouse gas emissions. With respect to aviation energy, there are mainly two types of options: one for propulsion options, including electric and hybrid power, and another for aviation energy options, including drop-in alternative jet fuel, liquid natural gas, and hydrogen. Drop-in alternative jet biofuel is considered the current promising available choice due to the no requirement for modifications in the aircraft with engine and infrastructure [1].

Alternative drop-in fuels should involve non-fossil hydrocarbon fuels with the same chemical structure with compatibility of blending conventional jet fuels [2]. The feedstocks should have the ability to mitigate CO_2eq emissions and large-scale output. Cellulosic straws derived from wheat, corn, rice, and bean have become significant advantages as a biomass source with abundant annual output.

The limited available volume of alternative jet biofuels is a limitation of feedstock and high cost. It is therefore important to continue exploring alternative routes for producing sustainable aviation fuels, which are not only economically competitive but also offer attractive savings of GHGs emissions. In compliance with ASTM standards, cellulosic straws can produce jet biofuel by Fischer–Tropsch pathway [3], alcohol-to-jet fuel (ATJ) pathway [4], and synthesized iso-paraffinic kerosene (SIP) pathway. ATJ and SIP are feasible technical routes for sugar-rich feedstock [5]. Fischer–Tropsch (FT) can obtain a wide variety of lignocellulosic biomass, but Fischer–Tropsch synthesis must overcome the cost barrier to face the existing technologies and to reach the market requirements [6]. The aqueous-phase conversion of lignocellulosic biomass to bio-jet fuel has attracted worldwide attention in recent years due to the mild operating condition and broad feedstocks [7]. The platform molecules (furfural, LA) could be derived from hydrolyzation from lignocellulosic biomass. The aldol condensation pathway followed by the hydrogenation could produce hydrocarbon biofuel whose carbon chain length is controlled in the jet fuel range.

The main objective is to evaluate the possible GHGs reduction and to highlight the impact of key parameters on life-cycle GHGs emission results. In this study, a quantitative assessment model has been established and can achieve uncertainty analysis and balance contradictory factors in the application of cellulose straw with sustainable biofuel benefits. The results would enhance the interest in both LCA assessment and CO_2 sequestration with sustainable biofuel benefits. For improving LCA-based methodology in the existing calculation approaches, the methodology in the flight stage has been improved in compliance with the whole flight envelope. Feedstock cultivation effects are assessed by local and global uncertainty analysis. The approach adopted to quantify land release effects is evaluated to show the potential contribution to GHGs emissions. The possible pathways for significant GHGs emission reductions were investigated in hydrogen production and CCUS (CO_2 capture utilization and storage) effect.

2. Method

2.1. Goal Definition and System Boundary

The objectives are to compare cellulose jet fuel with traditional jet fuel in terms of energy consumption and GHGs, and thus the assessment includes the total energy consumption (EC) and greenhouse gas emissions (GHGs). The functional units of energy consumption and GHGs emissions have been defined on per kg load and per km flight range. The GHGs, including carbon dioxide (CO_2), methane (CH_4), and nitrous oxide (N_2O), are all calculated as equivalent to 100 years of global warming potentials as gCO_2e/MJ, while volatile organic compounds (VOCs), CO, and NOx and particulate matter diameter (PM_{10} and $PM_{2.5}$) are involved in GHGs as a contrast.

Coupling the LCA approach and specific characteristics of cellulose jet fuel, cellulose jet fuel includes the feedstock stage, fuel stage, and flight stage. The initial system boundary of cellulose jet fuel has the ability of flexible options with or without cultivation, as shown in Figure 1.

In the feedstock stage of cornstalk, beanstalk, wheat straw, and rice stalk, the system boundary starts from cultivation and includes cultivation, harvesting, and transportation. For agriculture residue, the system boundary is defined to start from harvesting. In the cultivation module, the use of chemical fertilizers and herbicides was involved in energy consumption and GHGs, and the impact of land release was involved in GHGs assessment.

In the fuel stage, the refining stage includes the refining process and transportation and distribution to the airport. The refining process complies with the practical refining technology [8], which includes the hydrolysis sub-process, condensation sub-process, and hydrogenation sub-process. The hydrolysis sub-process includes hemicellulose for furfural and cellulose for levulinic acid. The condensation sub-process achieves oxygenate precursors by aldol condensation reaction between furfural and LA. The hydrogenations sub-process aims to remove heteroatom for hydrocarbon fuel by upgrading hydrotreatment.

In the flight stage, civil aircraft with associated engines are classified into six types. The typical civil aircraft with associated engines include single-aisle (SA 737-800, CFM56-7B27), small twin-aisle (STA 787-8, GEnx-1B67), large twin-aisle (LTA777-200 GE90-85B), large quad (LQ A380 Trent 970-84), regional jet (RJ ERJ-145 AE3007A2), and business jet (BJ G550 BR700-710C4-11). Cellulose jet fuel is considered drop-in jet fuel, which does not influence the lifetime of civil aircraft with associated engines.

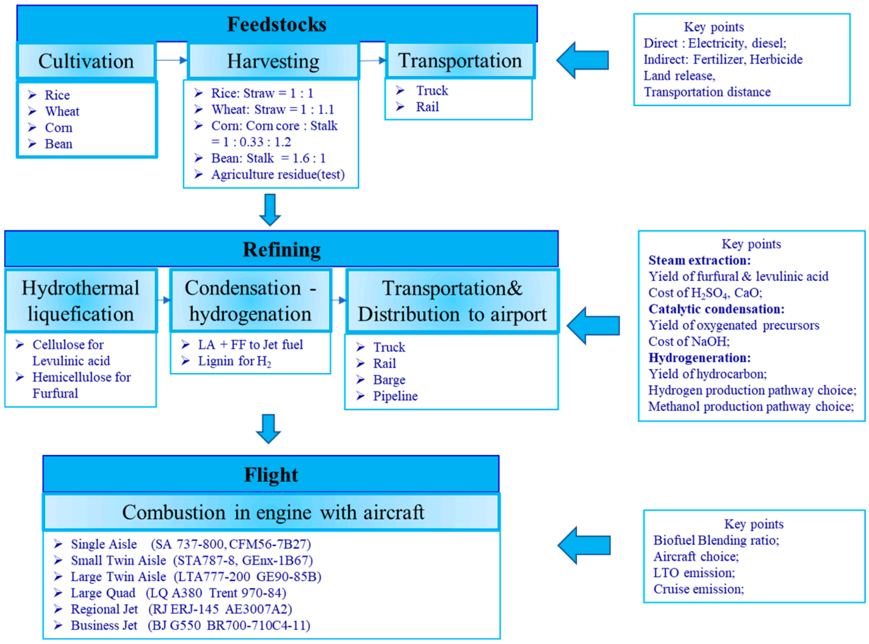

Figure 1. System boundary of cellulose jet fuel with the traditional jet fuel.

Electricity utilization is based on the consumption of fossil fuel and renewable energy in China. The hydrogen utilization can be chosen from solar energy, biomass, nature gas, or coal. Methanol utilization includes biomass, natural gas, or coal. The infrastructures of fossil fuel (petroleum, coal, natural gas) and electric power stations were not involved in the system.

The whole life cycle of traditional jet fuel starts from the well (crude oil) to the wheel (combustion in the engine). For jet biofuel, WTW (the whole life cycle) includes the cultivation of feedstock, refining jet fuel, and combustion in flight. WTP includes the feedstock stage (cultivation, harvesting, and transportation) and refining stage (hydrothermal liquefication, condensation–hydrogenation, transportation, and distribution to the airport). PTW includes the combustion in the engine with aircraft.

2.2. Cellulose Jet Fuel Computational Framework

According to the system boundary in compliance with functional units, the computational framework is integrated into three sub-models and three modules, which include the feedstocks model, fuel model, flight model, electricity module, hydrogen module, and methanol module. There are two flow lines to link the models. The mass flow complies with energy consumption related to final mass product (kg), while energy flow complies with energy consumption related to final energy yield (MJ).

In the feedstock model, the energy consumption of raw materials includes direct energy consumption and indirect energy consumption. Indirect energy consumption mainly comes from the use of chemical fertilizers and herbicides, while direct energy consumption includes electricity and power consumption in the process of planting, harvesting, and transportation. The impact of land release complies with the number of nitrogen fertilizers.

$$N_2O \text{ release (g/kg straw)} = \text{Input fertilizers}_{\text{nitrogen}} \text{ (g/kg)} \times \text{emission factor}_{\text{nitrogen}} \text{ (g/kg fertilizer)} \times \text{straw (kg)/straw(kg)} + \text{grain(kg)}.$$

In the refining model, based on the technical route of aqueous-phase conversion of lignocellulose biomass to bio-jet fuel [7,9], the hydrolysis of feedstock is hydrolyzed by two steps for the production of furfural and LA from hemicellulose and cellulose, respectively. The oxygenated precursors are formed by aldol condensation of furfural and LA with a basic catalyst and then are hydrotreated into jet biofuel via a series of hydrogenation, dehydration, and isomerization processes. The lignin is used for hydrogen production by gasification with steam output. The mass flow of cellulose jet fuel is given in Figure 2. The main product is normal and isomeric C8–C15 long-chain alkanes, while by-products include hydrogen and steam.

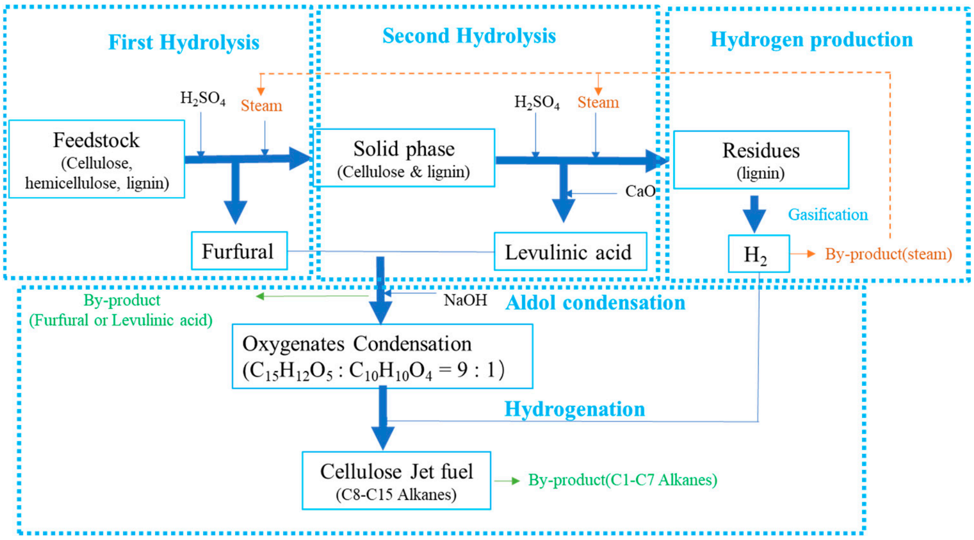

Figure 2. Process diagrams of cellulose jet fuel via aqueous-phase conversion.

In the flight module (LTO and Cruise), emissions affecting surface air quality are assessed over a standard landing–take-off (LTO) cycle and a cruise based on flight range limitation. On the basis of flight envelope, emissions were calculated by distance-weighted average in a full envelope, including LTO cycle and cruise. Energy consumption and GHGs emission are calculated per unit load and per unit flight range on the assumption of the maximum range.

The emission performance and fuel properties were tested by the lean premix pre-evaporation (LPP) platform in comparison with alternative jet fuel with the traditional jet fuel in energy consumption and GHGs. The emissions have been tested at power settings of a single aisle at reference meteorological conditions at temperature (15 °C), absolute humidity (0.00629 kg water/kg dry air), and pressure (101,325 pa). The GHGs covered in this analysis include carbon dioxide (CO_2), methane (CH_4), and nitrous oxide (N_2O) and also CO, volatile organic compounds (VOCs), mono-nitrogen oxides (NOx), sulfur oxides (SOx), and particulate matter diameter (PM_{10} and $PM_{2.5}$). The transfer coefficients from the test to the other types are established by coupling the characteristics of aircraft with the associated engine and average transfer coefficients collected in literature(reference), given in Table 1.

The emissions were calculated by distance-weighted average in a full envelope, including LTO and cruise. LTO modes include take-off (thrust 100%, 0.7 min), climb (thrust 85%, 2.2 min), approach (thrust 30%, 4 min), and taxi/idle (thrust 7%, 26 min) [10].

The cut-off criterion is set at less than 1% on the LCA results as iterative convergence. Carbon sequestration is based on the carbon content in jet biofuel, which complies with the following equation:

$$\text{carbon sequestration} = -\text{biofuel blending ratio} \times \text{fuel consumption (kJ/kg payload.km)} \times \text{carbon (\%/kJ biofuel)} \times 44/12.$$

In the whole life cycle of jet fuel, inputs and outputs related to the materials have been calculated by the mass allocation method as the contribution to energy consumption and GHGs. The electricity utilization in the whole life cycle shares the emissions and energy consumption by energy allocation on jet fuels and by-products.

GHGs comply with the mass allocation method, while energy consumption complies with the energy allocation method.

Table 1. Emission using cellulose jet fuels compared with RP-3.

Emission	Alternative Jet Fuel	LPP Burner (CJF/RP-3 Test)		Aircraft-Single Aisle (CJF/RP-3 Simulation)		Aircraft-Small Twin Aisle, Large Twin Aisle, Large Quad (CJF/RP-3 Simulation)		Aircraft-Regional Jet, Business Jet (CJF/RP-3 Simulation)	
	Blending ratio	LTO	Cruise	LTO	Cruise	LTO	Cruise	LTO	Cruise
CH_4	100%	0.38	0.28	0.38	0.28	0.52	0.38	0.34	0.25
	50%	0.80	0.30	0.80	0.30	0.71	0.27	0.20	0.52
N_2O	100%	1.00	1.00	1.00	1.00	1.00	1.00	1.00	1.00
	50%	1.00	1.00	1.00	1.00	1.00	1.00	1.00	1.00
CO_2	100%	0.999	0.999	0.999	0.999	0.999	0.999	0.999	0.999
	50%	0.999	0.999	0.999	0.999	0.999	0.999	0.999	0.999
UHC	100%	0.38	0.28	0.38	0.28	0.52	0.38	0.34	0.25
	50%	0.30	0.80	0.30	0.80	0.71	0.27	0.20	0.52
CO	100%	1.38	0.88	1.38	0.88	1.65	1.05	1.17	0.75
	50%	2.60	0.90	2.60	0.90	2.47	0.86	2.37	0.82
NO_x	100%	1.79	0.56	1.79	0.56	1.74	0.55	1.96	0.61
	50%	1.38	0.91	1.38	0.91	1.39	0.91	1.45	0.95
PM	100%	0.80	0.80	0.80	0.80	0.16	0.16	0.22	0.22
	50%	0.76	0.76	0.76	0.76	0.65	0.65	0.81	0.81
SOx	100%	0	0	0	0	0	0	0	0
	50%	0.51	0.51	0.51	0.51	0.51	0.51	0.51	0.51

2.3. Inventory Data

The main inventory data is derived from the original Chinese government data release [11,12] and the Beihang-AF3E model [1,13]. Petroleum jet fuel in the exploration and recovery process, as well as the refinery process, were collected [14,15], as given in Table 2.

LCI in the feedstock stage is derived from (http://zdscxx.moa.gov.cn), including the growth rate of grain, the ratio of grain to straw, and the amounts of fertilizer, pesticide, and herbicide. LCI in the fuel stage is based on practical pilot-scale refining [7–9]. Based on the contents of cellulose, hemicellulose, and lignin in feedstock, the yield of furfural is 0.385 g/g while that of LA is 0.259 g/g [16]. For the process of lignin to hydrogen, the yield is 35.5 g/kg [17].

H_2SO_4 acid is designed to achieve the yield of furfural and LA, while lime was used to adjust the pH value to deposit the produced $CaSO_4$. For aldol condensation reaction with hydrogenation, the yield of bio-jet fuel is 0.664 kg/kg FF [18].

LCI in the flight stage, traditional jet fuel derived from petroleum, HC, CO, and NOx emissions were selected from the ICAO databank, while CH_4, N_2O, and SOx emission were selected from AAFEX (Alternative Aviation Fuel Experiment) and AEDT (Aviation Environmental Design Tool) in NASA databank [11].

Cutoff criteria require the exclusion of unit processes and inputs that cumulatively contribute less than 3% based on mass, energy, and GHGs, respectively.

Table 2. The inventory in feedstock and fuel stage.

Feedstock Stage		Energy		Material, g/kg				Land Release	
Cultivation	**Feedstock**	**Electricity kwh/t**	**Diesel g/kg**	**N**	**P_2O_5**	**K_2O**	**Pesticides/ Herbicide**	**CH_4 kg/hm^2**	**N_2O kg/kgN**
	Rice	127.3–151.4	5.2–32.2	6.34	1.76	3.32	1.025	218	0.01
	Wheat	127.3–151.4	5.2–32.2	16.95	1.63	0	1.025	-	0.01
	Corn	44.3–77.9	4.4–13.9	11.08	0.57	0.37	0.275	-	0.01
	Bean	44.3–77.9	4.4–13.9	2.99	1.5	3.29	0.275	-	0.01
	Agriculture	-	-					-	-
Harvesting		7–22	0.5–2.4						
Transportation	25–50 km		0.02 kg/(t·km)						
Fuel stage		Electricity	Thermal heat	H_2	CH_3OH	CaO	H_2SO_4		
Hydrolysis/Aldol condensation/ Hydrotreating	FF 0.385 g/$g_{hemicellulose}$ LA 0.259 g/$g_{cellulose}$ H_2 0.105 g/g_{lignin}	234.73 MJ/$kg_{jet\ fuel}$	71.54 MJ/$kg_{jet\ fuel}$	0.142 g/$g_{jet\ fuel}$	28.43 g/kg_{straw}	279.41 g/kg_{straw}	503.92 g/kg_{straw}		

3. Results and Discussion

3.1. Feedstocks Stage

The feedstock stage is further classified into cultivation, harvesting, handling and storage, and transportation. Compared with the boundary effects, agriculture residue initiated from harvesting without the cultivation sub-stage. For energy consumption, the cultivation sub-stage includes the direct energy consumption related to electricity and diesel in the process of plant and maintenance and indirect energy consumption related to fertilizer, insecticide, and herbicide in the production. For GHGs emissions, the cultivation sub-stage includes the land release integrated with GHGs in energy consumption.

In the feedstock stage, agriculture residue makes the advantage in lowest energy consumption due to no allocation of energy consumption and GHGs emissions in the cultivation sub-stage, given in Figure 3. In the cultivation sub-stage, the direct energy consumption and indirect energy consumption are allocated according to the weight ratio of straw to grain. Of the four types of grain straw, beanstalk performs the lower energy consumption due to the low allocation of energy consumption derived from the lowest weight ratio of straw to grain, while wheat straw conducts the highest energy consumption. The energy consumption in the cultivation sub-stage occupies the total energy consumption in the feedstock stage: 87.7% rice straw, 87.2% wheat straw, 77.3% cornstalk, and 68.8% beanstalk, respectively. Indirect energy consumptions derived from fertilizer, insecticide, and herbicide are in the range of 20–35%, while direct energy consumptions are in the range of 42–62%. In comparison with the cultivation sub-stage, the energy consumptions in harvesting and transportation are around 0.24 MJ/kg straw.

In GHGs, rice farmland is one of the important sources of methane (CH_4) emissions due to wetland conditions [19]. As a result, rice straw conducts the highest GHGs emission than the other feedstock. The land release of rice straw takes up above 80% of total GHGs emissions while the others in land release occupy 20.3% wheat straw, 13.8% corn stove, and 8.3% beanstalk in the feedstock stage, which indicated that land release could not be ignored in the utilization of bio-feedstock.

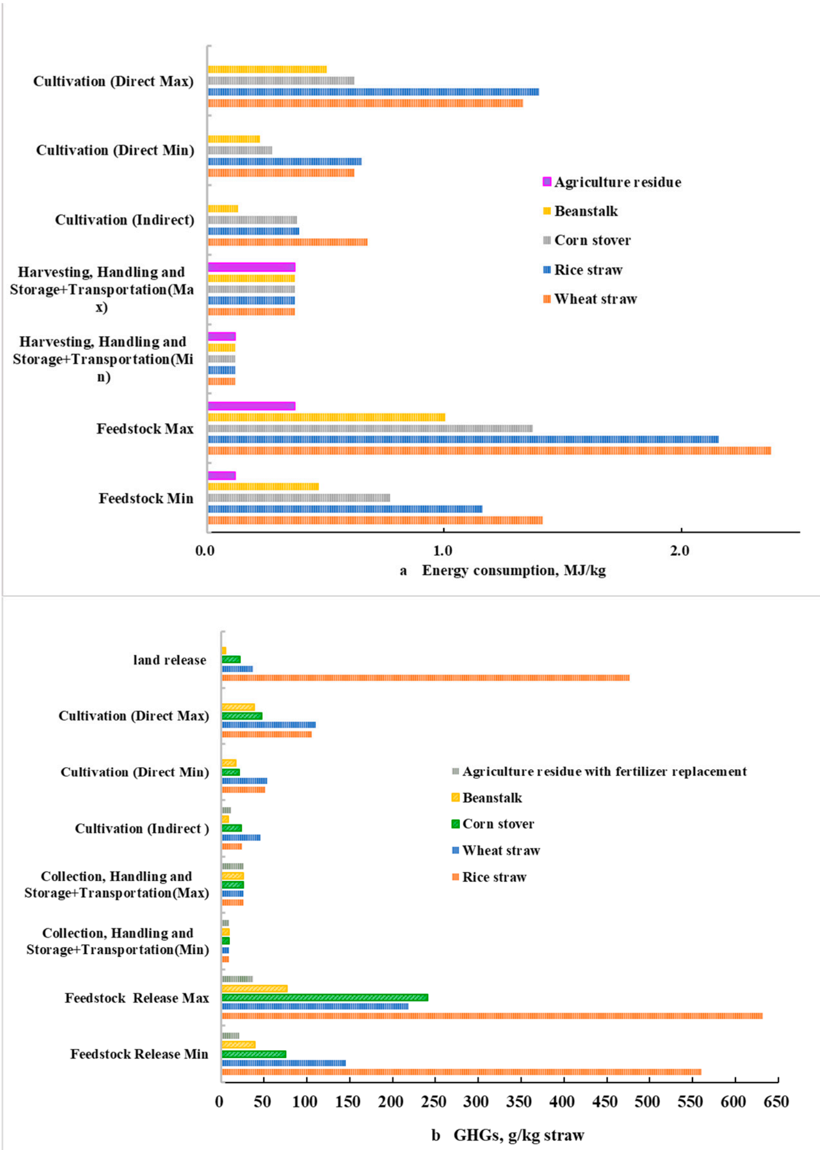

Figure 3. Energy consumption (**a**) and GHGs (**b**) in the feedstock stage.

Farmland is an important source of N_2O emission derived, accounting for about 90% of the total N_2O emission in the biosphere. Nitrogen fertilizer utilization occupies the most important part. Agricultural N_2O emission includes direct emission and indirect emission. Among them, direct emission refers to the discharge caused by the application of nitrogen fertilizer, and indirect emissions include atmospheric nitrogen deposition, leaching, and runoff emissions. In compliance with fertilizer utilization requirements and the ratio of grain to straw, the sequence of GHGs emissions in cultivation is rice straw, wheat straw, cornstalk, beanstalk, and agriculture residue. Except for agriculture residue without GHGs emission allocation in cultivation, beanstalk takes the advantage in GHGs emissions due to the low cost of fertilizer, electricity, and diesel fuel.

3.2. *Refining Stage*

In the refining stage, feedstock could hydrolyze to produce furfural (0.385 g/g hemicellulose), levulinic acid (0.259 g/g cellulose) under the acid condition in compliance with the contents of cellulose, and hemicellulose in rice straw, wheat straw, corn stove, beanstalk, and agriculture residue. Lignin could produce hydrogen (0.0355 g/g lignin) by pyrolysis and gasification.

By the aldol condensation, furfural and levulinic acid produce C10–C17 oxygen-containing compounds in alkali aqueous solution. C8–C16 hydrocarbon as a jet biofuel was obtained by hydrodeoxidation and hydrodeoxidation/isomerization reaction.

The main input of materials are methanol and hydrogen, and the main input of energy is electricity and heat energy. Based on the choice of coal for methanol and lignin for hydrogen, the impact of feedstock has been investigated in the total energy consumption and GHGs, given in Figure 4. The agriculture residue conducts the lower GHGs emission and energy consumption due to the appropriate content distribution of cellulose, hemicellulose, and lignin. Corn stoves performed with lower GHGs emissions and energy consumption in comparison with wheat straw, rice straw, and beanstalk. The energy consumptions are in the range of 1100–1420 MJ/kg jet fuel while the GHGs emissions are in the range of 16.8–17.6 GHGs g/kg jet fuel.

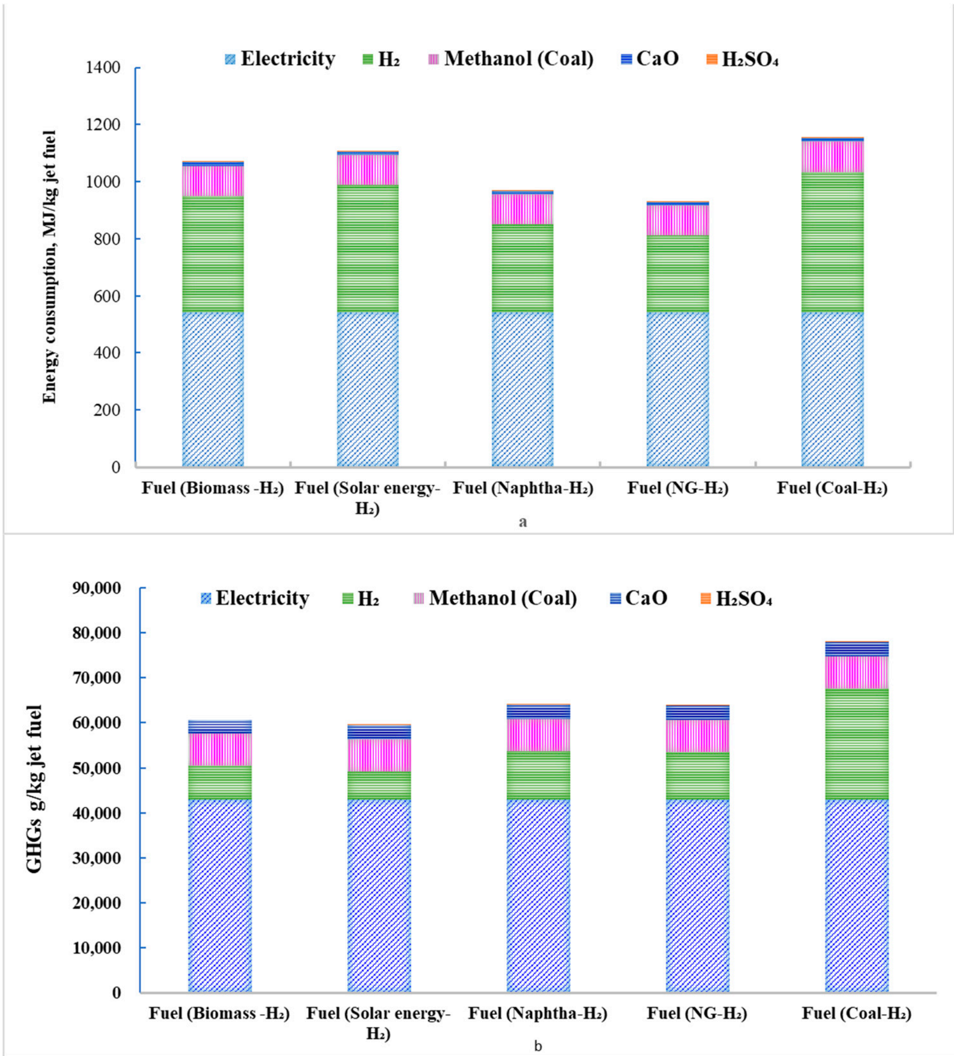

Figure 4. Energy consumption (**a**) and GHGs (**b**) of various feedstock in fuel stage (Coal for methanol and lignin for hydrogen).

For optimization of the energy consumption unit and GHGs emission unit in the fuel stage, the main units have been investigated based on agriculture residue, given in Figure 5. No matter which kind of hydrogen pathway choice, electricity occupies the first in GHGs emission in the fuel stage, which conduct above 50% GHGs emission. The integrated electricity and hydrogen share above 70% GHGs emissions in the fuel stage. In comparison with biomass for hydrogen, solar energy for hydrogen could benefit GHGs emissions but with higher energy consumption, while natural gas for hydrogen has an advantage in reduction of energy consumption but with higher GHGs emissions.

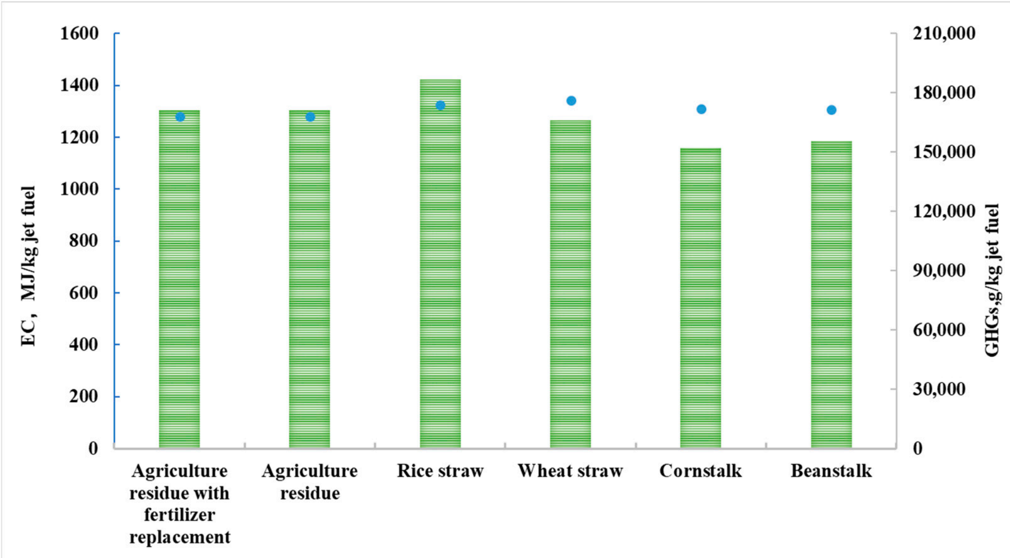

Figure 5. Energy consumption and GHGs of agriculture residue in fuel stage.

The integration of electricity and hydrogen shares most of the energy consumption and GHGs in the fuel stage. The third energy consumption unit and GHGs unit is the methanol unit. The uncertainty analysis of electricity, hydrogen, and methanol is in Section 3.4.

3.3. Flight Stage

GHGs emissions from engines in aircraft comply with a function of fuel consumption and engine efficiency, which is related to the combustor performance, including combustor temperature distribution, fuel-to-air ratio, and pressure. Aircraft engines are usually designed for optimum cruising performance, resulting in a less efficient LTO cycle. Therefore, GHGs emissions during the whole flight envelope could be classified into LTO cycle and cruise due to characterized different emission performances [20] and shown in Supplement Material Table S1.

The emissions of alternative fuel with 50% and 100% blend were investigated by the LPP burner platform in comparison with conventional jet fuel at LTO and cruise conditions. By similarity criterion to conform to the condition of the engine in a single aisle, the experimental emission data have been collected at LTO condition and cruise condition. Integrating emission characteristics of different types of engine aircraft with tests [1,11], the emissions of alternative fuels performance have been simulated, as given in Table 2, including carbon dioxide (CO_2), methane (CH_4), and nitrous oxide (N_2O), CO, UHC, particulate matter diameter (PM), and SOx.

As for the LTO cycle, cellulose jet fuels, compared with traditional jet fuel, have less PM, UHC, and CH4 emissions, while NOx emission increases. In the cruise cycle, cellulose jet fuels, compared with traditional jet fuel, have less PM, CH4, UHC, and NOx emissions. The emissions of PM_{10}, $PM_{2.5}$, and SO_2 decrease obviously in the combustion stage. Cellulose jet fuel contains no aromatic and no sulfur in comparison with RP-3, and the results are entirely consistent with the reduction of UHC, PM, and SOx. The results are coincident with the low sulfur content, low C/H ratio, and low aromatic hydrocarbon content in alternative fuels.

For assessment of the emissions during the whole flight, the total emissions were calculated by distance allocation, which complies with the distance distribution in LTO and cruise. From the view of engine and aircraft effects on GHGs emissions in the flight stage, cellulose jet fuel blending decreases the GHGs emission slightly. However, obvious differences can be found in six types of engine aircraft. The large twin-aisle aircraft shows the least emissions at CHJ 0.50 g/kg·km, RP-3 0.52 g/kg·km than business jet CHJ 2.37 g/kg·km, RP-3 2.27 g/kg·km, as given in Figure 6.

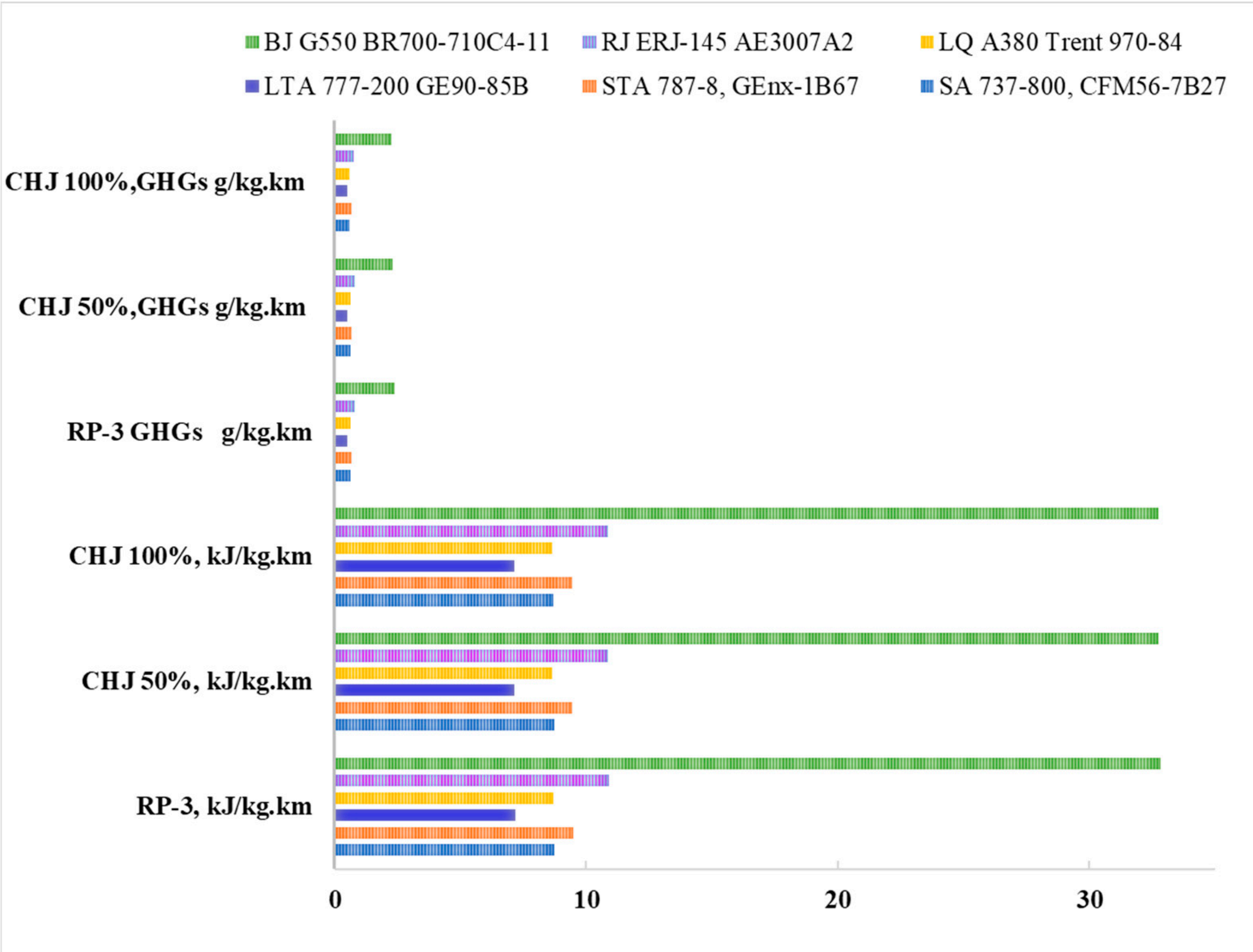

Figure 6. Flight stage Energy consumption and GHGs.

For energy consumption, the large twin-aisle aircraft shows the least energy consumption at CHJ 7.15 kJ/kg·km, RP-3 7.17 kJ/kg·km than business jet CHJ 32.75 kJ/kg·km, RP-3 32.85 kJ/kg·km due to high engine efficiency and large payload.

3.4. Uncertainty Analysis in WTW

In the whole life cycle assessment, GHGs of agriculture residue is 17.9 gCO_2e/MJ while petroleum-based jet fuel is 90.2 gCO_2e/MJ. From total energy and fossil fuel consumption, traditional jet biofuel conducted less fossil fuel consumption, given in Figure 7. The order of GHGs in WTW is agriculture residue < corn stover < beanstalk < wheat straw < rice straw.

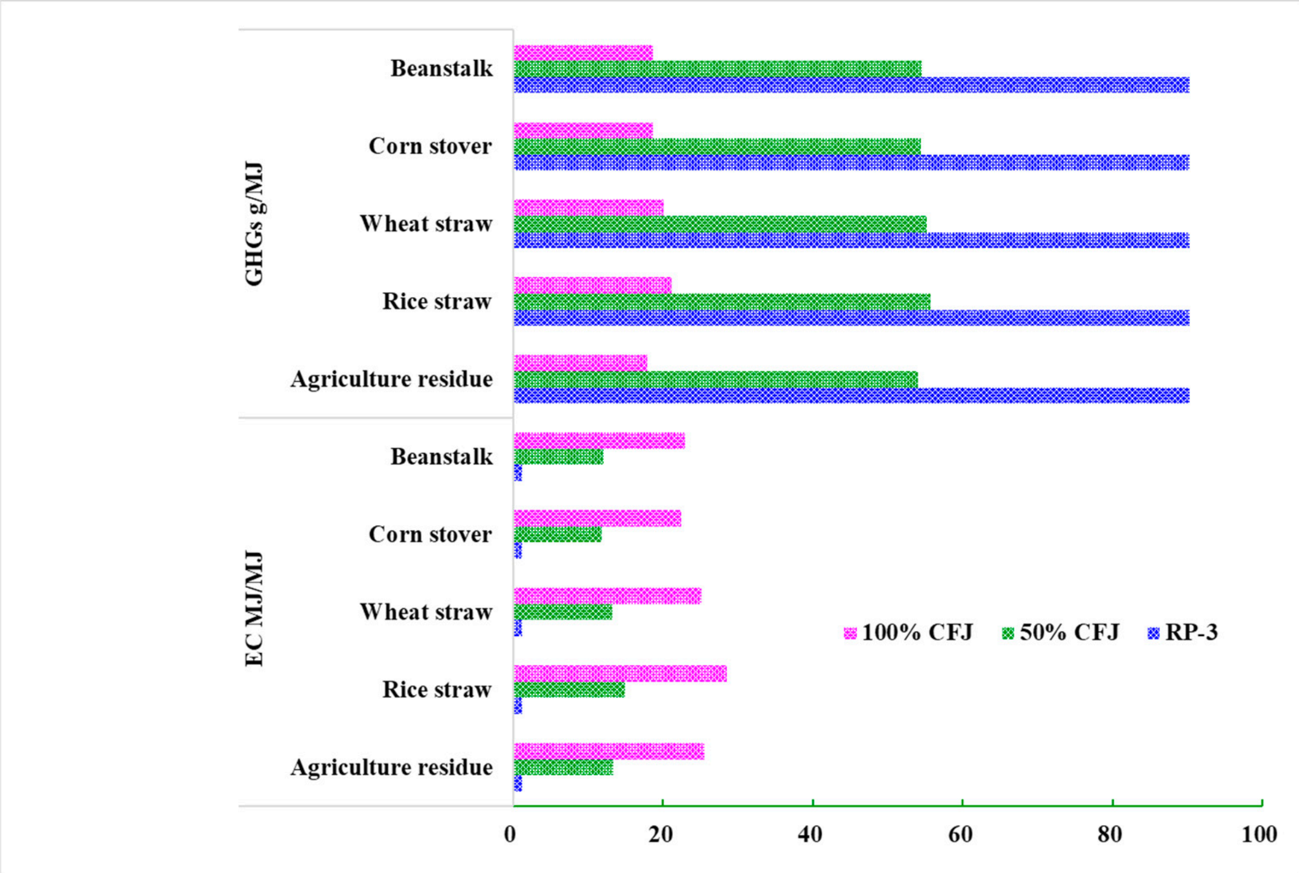

Figure 7. Total energy consumption and GHGs in whole life cycle.

Global sensitivity analysis aims at identifying how the uncertain input of a component contributes to the variability of the property output. There are two different types of sensitivity analysis involved, including local sensitivity analysis and global sensitivity analysis. The local sensitivity analysis is evaluated at the stage level, and the global sensitivity analysis is evaluated during the whole life cycle.

For feedstock uncertainty by local sensitivity analysis, GHGs emissions present significant differences in the feedstock stage. However, as the emissions in the flight stage contributed around 80% while those in the feedstock stage and fuel stage contributed around 20%, the impact factors on GHGs emission in the WTP stage contribute insensitive to the total GHGs emission in WTW by global sensitivity analysis, as given in Figure 8. For agriculture residue use change, fertilizer enhancement should contribute to the increase of GHGs, but only a slight impact can be shown. However, the land release conducted obviously to the total GHGs emission for rice straw, which indicated that land release should involve in the LCA.

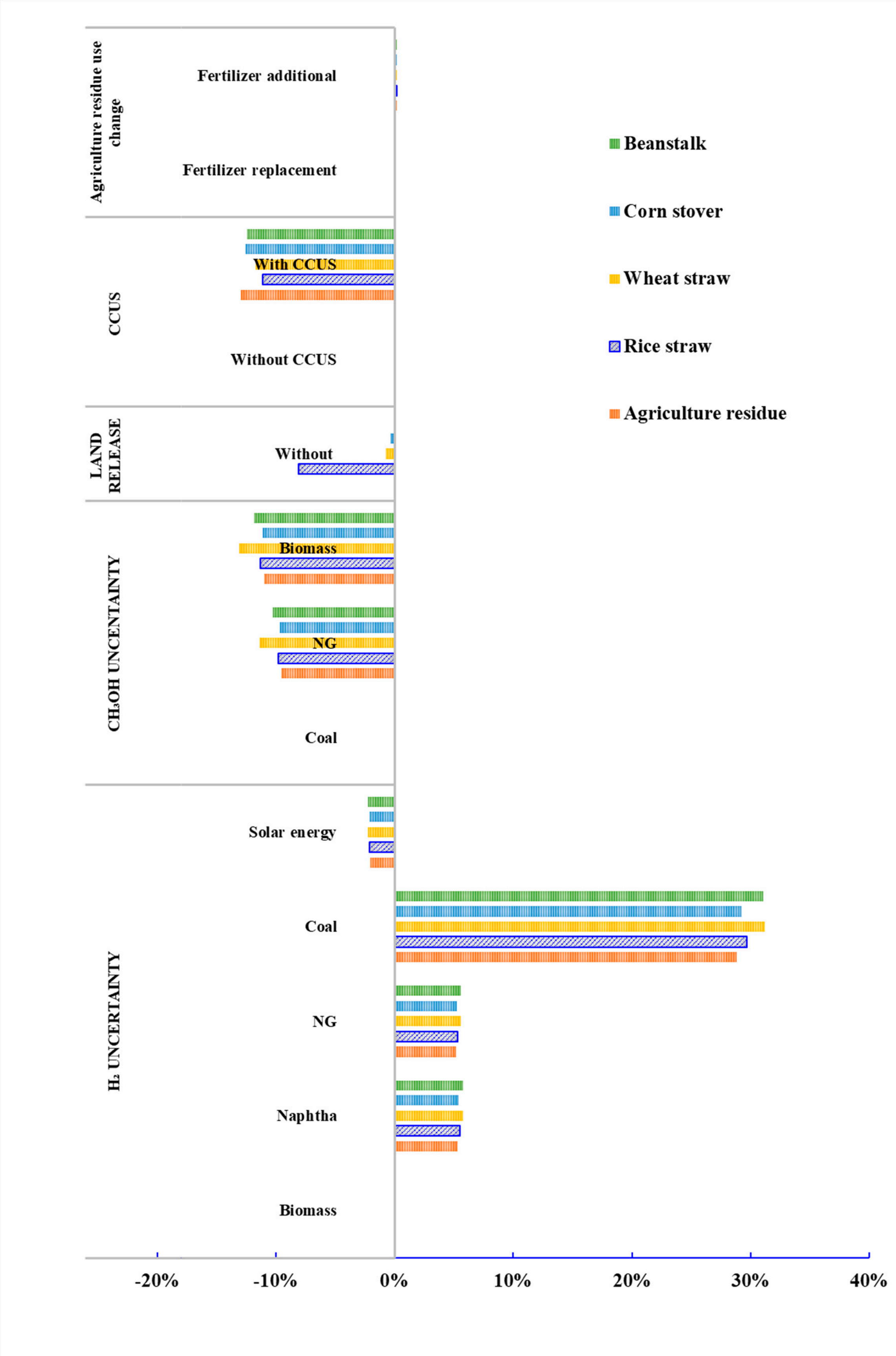

Figure 8. Uncertainty analysis at WTW level.

For hydrogen production uncertainty, naphtha, coal, and natural gas could enhance GHGs emissions except for solar energy compared with biomass. Coal for hydrogen increased 28.8–31.2% GHGs emissions, which is conducted sensitively to the total GHGs emission in WTW. For methanol production choice, biomass for methanol performs the lowest GHGs emission at 5469 GHGs g/kg than natural gas at 7669 GHGs g/kg and at coal 17,756 GHGs g/kg, which also conducted sensitively to the total GHGs emission in WTW. For CCUS effects on electricity, the results present that the GHGs emission reduction in electricity could benefit the reduction of the total GHGs emission in WTW.

4. Conclusions

The aqueous-phase conversion of lignocellulosic biomass to bio-jet fuel has shown a reduction in GHGs compared with petroleum-based jet fuel. The integration of electricity and hydrogen contributes to most of the energy consumption and GHGs in the fuel stage. The land release could not be ignored in the utilization of bio-feedstock. In comparison with biomass for hydrogen, solar energy for hydrogen could benefit GHGs emissions but with higher energy consumption, while natural gas for hydrogen has an advantage in reduction of energy consumption but with higher GHGs emissions. The results present that the GHGs emission reduction in electricity with CCUS could benefit the reduction of the total GHGs emission in WTW.

Supplementary Materials: The following supporting information can be downloaded at: https://www.mdpi.com/article/10.3390/aerospace10020129/s1, Table S1: Emission of different aircraft with different engine using conventional aviation fuel.

Author Contributions: Methodology, Z.L.; data curation and analysis, Z.L. and H.L.; writing—original draft preparation, Z.L. and H.L.; writing—review and editing, Z.L. and X.Y.; supervision, X.Y. All authors have read and agreed to the published version of the manuscript.

Funding: This paper was supported by the National High-tech Research and Development Program China (2018YFB1501505).

Institutional Review Board Statement: Not applicable.

Informed Consent Statement: Not applicable.

Data Availability Statement: The data presented in this study are available on request from the corresponding author. The data are not publicly available due to privacy.

Conflicts of Interest: The authors declare no conflict of interest.

References

1. Liu, Z.; Yang, X. Refining drop-in jet fuel coupling GHGs reduction in LCA with airworthiness in aero-engine and aircraft. *Catal. Today* **2020**, *353*, 260–268. [CrossRef]
2. Yang, X.; Guo, F.; Xue, S.; Wang, X. Carbon distribution of algae-based alternative aviation fuel obtained by different pathways. *Renew. Sustain. Energy Rev.* **2016**, *54*, 1129–1147. [CrossRef]
3. Fernanda, M.; Michailos, S.; Akram, M.; Cardozo, E.; Hughes, K.J.; Ingham, D.; Pourkashanian, M. Bioenergy with carbon capture and storage (BECCS) potential in jet fuel production from forestry residues: A combined Techno-Economic and Life Cycle Assessment approach. *Energy Convers. Manag.* **2022**, *255*, 115346. [CrossRef]
4. Guo, X.; Guo, L.; Zeng, Y.; Kosol, R.; Gao, X.; Yoneyama, Y.; Yang, G.; Tsubaki, N. Catalytic oligomerization of isobutyl alcohol to jet fuels over dealuminated zeolite Beta. *Catal. Today* **2020**, *368*, 196–203. [CrossRef]
5. Tanzil, A.H.; Brandt, K.; Wolcott, M.; Zhang, X.; Garcia-Perez, M. Strategic assessment of sustainable aviation fuel production technologies: Yield improvement and cost reduction opportunities. *Biomass Bioenergy* **2021**, *145*, 105942. [CrossRef]
6. Santos, D.; Goncalves, R.; Alencar, A.C. Biomass-derived syngas production via gasification process and its catalytic conversion into fuels by Fischer Tropsch synthesis: A review. *Int. J. Hydrogen Energy* **2020**, *45*, 18114–18132. [CrossRef]
7. Li, Y.; Chen, L.; Zhang, X.; Zhang, Q.; Wang, T.; Qiu, S.; Tan, J.; Li, K.; Ma, L. Process and Techno-economic Analysis of Bio-jet Fuel-range Hydrocarbon Production from Lignocellulosic Biomass via Aqueous Phase Deconstruction and Catalytic Conversion. *Energy Procedia* **2017**, *105*, 675–680. [CrossRef]
8. Zhang, Q.; Li, Y.; Chen, G.; Wang, T.; Liu, Y.; Zhang, X.; Tan, J.; Li, K.; Ma, L. Material and Energy Conversion of Integrated 100 t/a-Scale Bio-Jet Fuel-Range Hydrocarbon Production System via Aqueous Conversion of Biomass. *J. Tianjin Univ. (Sci. Technol.)* **2017**, *50*, 13–18. (In Chinese) [CrossRef]

9. Wang, C.; Zhang, X.; Liu, Q.; Zhang, Q.; Ma, L. A review of conversion of lignocellulose biomass to liquid transport fuels by integrated refining strategies. *Fuel Process. Technol.* **2020**, *208*, 106485. [CrossRef]
10. Carter, N.; Stratton, R.; Bredehoeft, M.; Hileman, J. Energy and Environmental Viability of Select Alternative Jet Fuel Pathways. In Proceedings of the 47th AIAA/ASME/SAE/ASEE Joint Propulsion Conference & Exhibit, San Diego, CA, USA, 31 July–3 August 2011. [CrossRef]
11. A, L.; Wen, M.; Guo, F.; Yang, X. Life cycle assessment of algae based aviation fuel on basis of engine type and related aircraft. *J. Aerosp. Power* **2018**, *33*, 1315–1325. (In Chinese) [CrossRef]
12. Zhao, J.; Guo, F.; Yang, X. Research of sustainable feedstock for future alternative aviation fuels. *J. Beijing Univ. Aeronaut. Astronaut.* **2016**, *42*, 2378–2385. (In Chinese) [CrossRef]
13. Liu, Z.; Liu, C.; Han, S.; Yang, X. Optimization upstream CO_2 deliverable with downstream algae deliverable in quantity and quality and its impact on energy consumption. *Sci. Total Environ.* **2019**, *709*, 136197. [CrossRef] [PubMed]
14. Ou, X.; Zhang, X.; Chang, S. Scenario analysis on alternative fuel/vehicle for China's future road transport: Life-cycle energy demand and GHG emissions. *Energy Policy* **2010**, *38*, 3943–3956. [CrossRef]
15. Ou, X.; Zhang, X.; Chang, S. Alternative fuel buses currently in use in China: Life-cycle fossil energy use, GHG emissions and policy recommendations. *Energy Policy* **2010**, *38*, 406–418. [CrossRef]
16. Dong, S.; Huang, X.; Yang, X. Energy consumption for production of jet fuel precursors from cellulosic biomass by hydrothermal method. *J. Beijing Univ. Areonautics Astronaut.* **2022**, *48*, 620–631. (In Chinese) [CrossRef]
17. Wu, C.; Wang, Z.; Dupont, V.; Huang, J.; Williams, P.T. Nickel-catalysed pyrolysis/gasification of biomass components. *J. Anal. Appl. Pyrolysis* **2013**, *99*, 143–148. [CrossRef]
18. Huang, X.; Dong, S.; Yang, X. Energy consumption of condensation-hydrogenation process to prepare alkanes from lignocellulose biomass. *J. Beijing Univ. Aeronaut. Astronaut.* **2022**, *48*, 121–131. (In Chinese) [CrossRef]
19. Wang, Z.; Zhang, X.; Liu, L.; Wang, S.; Zhao, L.; Wu, X.; Zhang, W.; Huang, X. Estimates of methane emissions from Chinese rice fields using the DNDC model. *Agric. For. Meteorol.* **2021**, *303*, 108368. [CrossRef]
20. Qing, X. Research on the Atmospheric Evironment Impact Assessment from Aircraft Engine Emissions in Airport. Ph.D. Thesis, Nanjing University of Aeronautics and Astronautics, Nanjing, China, 2009. (In Chinese) [CrossRef]